Title	**Human ether-à-go-go gene potassium channels are regulated by EGFR tyrosine kinase**
Author(s)	**Wu, W; Dong, MQ; Wu, XG; Sun, HY; Tse, HF; Lau, CP; Li, GR**
Citation	**Biochimica Et Biophysica Acta - Molecular Cell Research, 2012, v. 1823 n. 2, p. 282-289**
Issued Date	**2012**
URL	**http://hdl.handle.net/10722/143374**
Rights	**NOTICE: this is the author's version of a work that was accepted for publication in Biochimica et Biophysica Acta. Changes resulting from the publishing process, such as peer review, editing, corrections, structural formatting, and other quality control mechanisms may not be reflected in this document. Changes may have been made to this work since it was submitted for publication. A definitive version was subsequently published in Biochimica et Biophysica Acta, 2012, v. 1823 n. 2, p. 282-289. DOI: 10.1016/j.bbamcr.2011.10.010**

BBAMCR-11-156R2

Human *ether-à-go-go g*ene potassium channels are regulated by EGFR tyrosine kinase

Wei Wu,[1] Ming-Qing Dong,[1] Xing-Gang Wu,[1] Hai-Ying Sun,[1] Hung-Fat Tse,[1] Chu-Pak Lau,[1] Gui-Rong Li[1,2]

[1]Department of Medicine, Li Ka Shing Faculty of Medicine, The University of Hong Kong, Pokfulam, Hong Kong, China
[2]Department of Physiology, Li Ka Shing Faculty of Medicine, The University of Hong Kong, Pokfulam, Hong Kong, China

Running title: EGFR kinase and hEAG1 channel regulation

Correspondence to

Dr. Gui-Rong Li, L4-59, Laboratory Block, FMB, The University of Hong Kong, 21 Sassoon Road, Pokfulam, Hong Kong, China

Tel: 852-2819-9513; Fax: 852-2855-9730; Email: grli@hkucc.hku.hk

Abstract
Human ether á-go-go gene potassium channels (hEAG1 or Kv10.1) are expressed in brain and various human cancers and play a role in neuronal excitement and tumor progression. However, the functional regulation of hEAG channels by signal transduction is not fully understood. The present study was therefore designed to investigate whether hEAG1 channels are regulated by protein tyrosine kinases (PTKs) in HEK 293 cells stably expressing hEAG1 gene using whole-cell patch voltage-clamp, immunoprecipitation, Western blot, and mutagenesis approaches. We found that the selective epidermal growth factor receptor (EGFR) kinase inhibitor AG556 (10 μM), but not the platelet growth factor receptor (PDGFR) kinase inhibitor AG1295 (10 μM) or the Src-family inhibitor PP2 (10 μM), can inhibit hEAG1 current, and the inhibitory effect can be reversed by the protein tyrosine phosphatase (PTP) inhibitor orthovanadate. Immunoprecipitation and Western blot analysis revealed that tyrosine phosphorylation level of hEAG1 channels was reduced by AG556, and the reduction was significantly countered by orthovanadate. The hEAG1 mutants Y90A, Y344A and Y485A, but not Y376A, and Y479A, exhibited reduced response to AG556. Interestingly, the inhibition effect of AG556 was lost in triple mutant hEAG1 channels at Y90, Y344, and Y485 with alanine. These results demonstrate for the first time that hEAG1 channel activity is regulated by EGFR kinase at the tyrosine residues Tyr_{90}, Try_{344}, and Try_{485}. This effect is likely involved in regulating neuronal activity and/or tumor growth.

1. Introduction

Human ether á-go-go gene potassium channels (hEAG1 or Kv10.1) are expressed in the nervous system [1,2] and various human cancers [3–6] and are believed to play a role in neuronal excitement [1,7] and tumor progression [3,4,6]. Knockdown of hEAG1 channels by hEAG1 siRNA suppressed cell proliferation in several human tumor cell lines [8], while activation of hEAGl channels by arachidonic acid enhanced cell proliferation in human melanoma cells [9]. Earlier studies demonstrated that hEAG1 was regulated by Ca^{2+}/calmodulin [10,11], calmodulin-dependent kinase II [12], and cyclic AMP [1], and membrane-associated guanylate kinase adaptor proteins [13]. Protein tyrosine kinases (PTKs), including both receptor PTKs (e.g. EGFR kinase, epidermal growth factor receptor kinase) and non-receptor PTKs (e.g. Src-family kinases), are important intracellular signals [14,15]. In addition to the mediation of cellular events such as cell growth, differentiation, embryonic development, metabolism, immune system function and oncogenesis [14,15], PTKs regulate ion channels activity [16,17], including K^+ channels [18–21], Na^+ channels [22], and Cl^- channels [23]. We recently found that human ether á-go-go related gene (hERG or Kv11.1) potassium channels were regulated by both EGFR kinase and Src-family kinases [19]; however, the potential regulation of the super-family hEAG1 channels by PTKs is unknown. The present study was therefore to determine whether and how hEAG1 channels stably expressed in HEK 293 cells are regulated by PTKs using whole-cell patch voltage clamp, immunoprecipitation, Western blot, and site-directed mutagenesis approaches. We found that the EGFR kinase inhibitor AG556, but not the Src-family kinase inhibitor PP2, inhibited hEAG1 current by decreasing tyrosine phosphorylation of the channel.

2. Materials and methods

2.1. Cell culture, mutagenesis, and gene transfection

The plasmid hEAGl/pTracer CMV [8] was generously provided by Dr. L. Pardo and was transfected into HEK 293 cells (ATCC, Manassas, VA). The HEK 293 cell line stably expressing hEAG1 channels were established as previously described [24,25], and selected with 800 μg/ml zeocin (Invitrogen, Hong Kong, China). The cell line was cultured in Dulbecco's modified Eagle's medium (DMEM, Invitrogen, Hong Kong) supplemented with 10% fetal bovine serum, 300 μg/ml zeocin.

The predicted potential tyrosine phosphorylation sites of hEAG1 channels were examined using the software NetPhos 2.0 (www.cbs.dtu.dk/cgi-bin). The mutant hEAG1 channels were generated using the QuickChange site-directed mutagenesis kit (Stratagene, La Jolla, CA, USA) following the manufacturer's instructions, and confirmed by full DNA sequencing analysis (Gene Centre, University of Hong Kong). The mutants Y90A, Y344A, Y376A, Y479A, Y485A, Y639A and Y639F were transiently expressed separately in HEK 293 cells using 10 μl of Lipofectamine 2000 with 4 μg of the plasmid in a 35 mm culture dish. The cells used for electrophysiology were seeded on a glasscover slip.

2.2. Solutions and chemicals

Tyrode solution contained (mM) NaCl 140, KCl 5.4, $MgCl_2$ 1.0, $CaCl_2$ 1.8, 4-(2-hydroxyethyl)-1-piperazineethanesulfonic acid (HEPES) 10.0 and glucose 10 (pH adjusted to 7.3 with NaOH). For whole-cell current recordings, the pipette solution contained (mM) KCl 20, Kaspartate 110, $MgCl_2$ 1.0, HEPES 10, ethyleneglycoltetraacetic acid (EGTA) 5, GTP 0.1, Na_2-phosphocreatine 5 and Mg-ATP 5 (pH adjusted to 7.2 with KOH). 3-(4-Chlorophenyl) 1-(1,1-dimethylethyl)-1H-pyrazolo[3,4-d] pyrimidin-4-amine (PP2) was purchased from Tocris (Bristol, UK). All other reagents were obtained from Sigma-Aldrich (St Louis, MO, USA). Stock solutions were made with dimethylsulfoxide (DMSO) for AG556 (100 mM), AG1295 (20 mM) and PP2 (10 mM). The stocks were divided into aliquots and stored at −20°C. Sodium orthovanadate stock solution (200 mM) was made with distilled water, and pH was adjusted to 9.0.

2.3. Electrophysiology

Cells on a coverslip were transferred to a cell chamber (0.5 ml) mounted on the stage of an inverted microscope (Diaphot, Nikon, Japan) and superfused at ~2 ml/min with Tyrode solution. Whole cell currents were recorded as described previously [24,25]. Borosilicate glass electrodes (1.2-mm OD) were pulled with a Brown–Flaming puller (model P-97, Sutter Instrument Co, Novato, CA) and had tip resistances of 2–3MΩ when filled with the pipette solution. A 3-M KCl–agar bridge was used as the reference electrode. The tip potential was zeroed before the patch pipette contacted with the cell. After a gigaohm seal was obtained by negative pressure, the cell membrane was ruptured by applying a gentle suction to establish whole cell configuration. Series resistance (Rs, 3–6MΩ) was compensated by 60–80% to minimize voltage errors. The liquid junction potential (13.5 mV) was not corrected throughout the experiment. Membrane currents were recorded using an EPC-10 amplifier and Pulse software (Heka Elektronik, Lambrecht, Germany). Command pulses were generated by a 12-bit digital-to-analog converter controlled by Pulse software. Current signals were low-pass filtered at 5 kHz and stored in the hard disk of an IBM compatible computer. All experiments were conducted at room temperature (22–23 °C).

2.4. Immunoprecipitation and Western blotting

The immunoprecipitation and Western blotting were performed following the procedure as described previously [19,20]. HEK 293 cells (~80% confluence) stably expressing hEAG1 channels were treated respectively with different compounds for 30 min at room temperature, and centrifuged (400×g for 10 min) at 4 °C. The cell pellet was then lysed with lysis buffer containing (mM) Tris 25, NaCl 150, NaF 1.0, EDTA 1.0, orthovanadate 1.0, phenylmethylsulfonyl fluoride 1.0, and 1% Na deoxycholate, 0.1% SDS, 1% Triton X-100, 1 μg/ml leupeptin, and 1 μg/ml aprotinin. Protein quantification of lysates was made using a protein assay reader (Bio-Rad Laboratories, Hercules, CA, USA), and diluted to equal concentrations.

Proteins were immunoprecipitated overnight at 4 °C using 2 μg of anti-KCNH1 (i.e. anti-hEAG1) antibody (NBP1-42816, Novus Biologicals, Littleton, CO, USA) and 100 μl of protein A/G beads (DAM 1460243, Millipore, Billerica, MA, USA). Immunoprecipitated proteins bound to pelleted protein A/G beads were washed thoroughly in PBS, denatured in Laemmli sample buffer, separated using SDSPAGE, and electroblotted onto nitrocellulose membranes. The immunoblots were probed with anti-phosphotyrosine antibody (1:1000, Cell Signaling Technology Inc., Danvers, MA, USA) overnight at 4 °C in a blocking solution containing 5% BSA in TBS and Tween 20, and subsequently treated with goat anti-mouse IgGHRP antibody (1:5000, Santa Cruz Biotechnology) for 2 h at room temperature. Blots were developed with enhanced chemiluminescence (ECL, Amersham Biosciences, Sweden) and exposed on an Xray film (Fuji Photo Film GmbH). The blots were then stripped and reprobed with the anti-hEAG1 antibody to determine total hEAG1 channel proteins. The film was scanned, imaged by a Bio-Imaging System (Syngene, Cambridge, UK), and analyzed via GeneTools software (Syngene).

2.5. RNA interference

Short interference RNA (siRNA) molecules targeting human EGFR (sc-29301) were purchased from Santa Cruz Biotech. This siRNA is a mixture of three target-specific 20–25 nucleotide siRNAs designed to knock down human EGFR gene expression. HEAG1-HEK 293 cells at 40–50% confluence were transfected with siRNA molecules at a total of 40 nM using Lipofectamine 2000 reagent (Invitrogen) in accordance with the manufacturer's protocol. The silencer negative control #1 siRNA (Ambion, #AM4611; Austin, TX), which contains no known target in mammalian genomes, was used as negative control. After 72 h of transfection, the cells were used for immunoprecipitation and Western blotting analysis as described above.

2.6. Statistical analysis

Data are expressed as means±S.E.M. Nonlinear curve-fitting was performed using Pulsefit (HEKA) and Sigmaplot (SPSS, Chicago, IL). Paired and/or unpaired Student's t-test was used as appropriate to evaluate the statistical significance of differences between two group means, and ANOVA was used for multiple groups. Values of $P<0.05$ were considered to be statistically significant.

3. Results

3.1. Effects of PTKs inhibitors on hEAG1 current

The PTKs effects on hEAG1 current were investigated by applying the highly selective EGFR kinase inhibitor AG556 [26], the selective platelet growth factor receptor (PDGFR) kinase inhibitor AG1295 [27], and the Src-family kinases inhibitor PP2 [28]. Fig. 1A shows the time course of hEAG1 current recorded at +50 mV (Fig. 1A) in the absence and presence of 10 μM AG556. AG556 gradually reduced the current. The inhibitory effect reached a steady-state level within 5 min upon AG556 exposure, and recovered rapidly on washout. Voltage-dependent hEAG1 current (Fig. 1B) was also inhibited by 10 μM AG556 (8 min), and the effect recovered on washout. Fig. 1C illustrates the mean values of current–voltage (I–V) relationships of hEAG1 current in the absence and presence of 10 μM AG556. The current was significantly suppressed at potentials from +30 to +60 mV (n=6, $P<0.01$ vs. control). Voltage-dependent variables (g) of hEAG1 current were calculated for each cell with I–V relationship curves as shown in Fig. 1C based on the formulation $g=I/(V_T-V_R)$, where I is the current at test potential (V_T), and V_R is the measured reversal potential (−70 mV). The normalized current (Fig. 2A) was fitted to a Boltzmann equation as described previously [18]. The half voltage ($V_{1/2}$) of activation of hEAG1 current was negatively shifted from 15.5±1.6 mV in control to 0.1±3.3 mV with 10 μM AG556 (n=4, $P<0.01$). The effect was reversed by washout (14.7±3.0 mV $P<0.01$ vs AG556). The slope factor was increased from 17.1±0.7 mV in control to 23.5±1.1 mV with 10 μM AG556 ($P<0.01$ vs control), and recovered on washout (18.0±0.4 mV).

Earlier studies reported that EAG channel current exhibited the property of holding potential-dependent activation, i.e. slower activation at hyperpolarization potentials [29,30]. We found that activation of hAEG1 current rapidly reached a steady-state level during 300-ms depolarization at holding potential of −50 mV, but not at a holding potential of −80 mV, in human bone marrow-derived mesenchymal stem cells [31], supporting the notion that the activation process of hEAG1 current depends on holding potential. Fig. 2B illustrates the hEAG1 current traces and voltage protocol (1-s conditioning holding potentials to between −100 and −20 mV, then step to a 300-ms test potential of +50 mV) used to evaluate activation time to 80% current amplitude [30] during control, in the presence of 10 μM AG556, and after washout (8 min). The time to 80% current activation decreased as the conditioning holding potential became more positive, and AG556 reversibly inhibited amplitude and time to 80% activation of hEAG1 current. The mean value of the time to 80% was significantly reduced with AG556 at all conditioning potentials (n=5, $P<0.01$ vs control). AG556-induced modification of hEAG1 kinetics recovered almost fully on washout (Fig. 2C). Fig. 3 illustrates the effects of the selective platelet growth factor receptor (PDGFR) kinase inhibitor AG1295, and the Src-family kinases inhibitor PP2 on hEAG1 current in representative cells. AG1295 (10 μM) or PP2 (10 μM) had no effect on hEAG1 current with 10 min exposure. The current (+50 mV) was 289±14 pA/pF in control and 287±11 pA/pF (n=8, P=NS vs control) after 10 μM AG1295. For PP2 group, the current was 302±14 pA/pF in control and 298±12 pA/pF (n=7, P=NS vs control) after 10 μM PP2. These results suggest that the EGFR kinase inhibitor AG556, but not PDGFR kinase inhibitor AG1295 or the Src-family kinase inhibitor PP2, inhibits hEAG1 current in HEK cells stably expressing hEAG1 gene.

3.2. Orthovanadate on AG556 effect

To exclude the possibility that the decrease of hEAG1 current by AG556 was mediated by a direct channel block, the PTP inhibitor orthovanadate was employed to examine whether the inhibitory effect of AG556 on hEAG1 current is through EGFR kinase inhibition (Fig. 4). Orthovanadate at 1 mM had no effect on hEAG1 current (n=5, data not shown); however, it significantly reversed the inhibitory effect of voltage-dependent hEAG1 current induced by AG556 (Fig. 4A). Fig. 4B displays the time-course of hEAG1 current recorded

at +50 mV in a typical experiment during control, in the presence of 10 μM AG556, and AG556 plus 1 mM orthovanadate. The inhibition of hEAG1 current by AG556 was rapidly countered by orthovanadate. Fig. 4C illustrates the mean percentage values of hEAG1 current at +50 mV during control, after the application of AG556, and AG556 plus orthovanadate. The current was reduced by 45.1±4.7% with 10 μM AG556 (n=8, P<0.01 vs control), and the inhibiting effect of AG556 was antagonized by 1 mM orthovanadate to 2.9±1.1% of control (n=8, P<0.01 vs AG566 alone). These results suggest that inhibitory effect of hEAG1 current by AG556 is likely mediated by EFGR kinase inhibition. Western blot analysis revealed that EGFR expression was significant in HEK 293 cells (Fig. 4D), consistent with previous report [32]. Fig. 5 shows that the modification of activation conductance (Fig. 5A) and voltage-dependent activation process (Fig. 5B and C) induced by the EGFR kinase inhibitor AG556 could be significantly countered by the PTP inhibitor orthovanadate.

3.3. Tyrosine phosphorylation level of hEAG1 channels

If the hEAG1 current reduction by AG556 is mediated by EGFR kinase inhibition, tyrosine phosphorylation level of hEAG1 channel protein should be reduced by this inhibitor. Fig. 6A and B shows the immunoprecipitation and Western blot images in hEAG1 HEK 293 cells treated with vehicle (control), 1 mM orthovanadate, 10 μM AG556, orthovanadate plus AG556, 10 μM PP2, or 100 ng/ml EGF. Tyrosine phosphorylation level of hEAG1 channel protein was reduced by AG556, and the reduction was antagonized by orthovanadate. No significant change was observed in cells treated with orthovanadate, EGF, or PP2. Fig. 6D illustrates the mean percentage values of pTyr-hEAG1 level relative to hEAG1 channel protein. Tyrosine phosphorylation level of hEAG1 channel protein was significantly decreased by AG556 (n=5–7, P<0.01 vs control), but not by PP2. These results indicate the hEAG1 channel activity is regulated by EGFR kinase, but not by Src-family kinases. Orthovanadate or EGF alone had no effect on the tyrosine phosphorylation level or the hEAG1 current (n=5, data not shown). This suggests that tyrosine phosphorylation level of hEAG1 channels is saturated under control conditions. Interestingly, tyrosine phosphorylation level was remarkably reduced in hEAG1-HEK cells transfected with 40 nM siRNA targeting EGFR (Fig. 6C and D), supporting the notion that the saturated tyrosine phosphorylation of hEAG1 channels is mediated by EGFR kinase.

3.4. Tyrosine phosphorylation sites of hEAG1 channels

To determine the molecular regulation sites of EGFR kinase, seven mutants at different tyrosine sites of hEAG1 channels were generated, including Y90A, Y344A, Y376A, Y479A, Y485A, Y639A and Y639F. The mutant Y639A or Y639F showed no functional currents (data not shown). This may suggest that Tyr_{639} is likely a critical amino acid residue in the C-terminus for maintaining functional hEAG1 channels and changes at Tyr_{639} may cause a significant conformational alteration leading to functional loss of hEAG1 channels.

Fig. 7A displays the inhibitory sensitivity of WT-hEAG1 and five other mutants to the EGFR kinase inhibitor AG556. With 10 μM AG556, similar inhibitory effect was observed in WT-hEAG1, and the mutants Y376A and Y479A; however, a reduced inhibition was observed in the mutants Y90A, Y344A and Y485A. Fig. 7B shows the current in a representative cell expressing the triple mutant gene with Y90A, Y344A and Y485A. The cells with triple mutant hEAG channel lost sensitivity to AG556. Fig. 7C illustrates the mean percentage values of AG556 inhibition for different mutant hEAG1 channels. AG556 at 10 μM reduced hEAG1 current (+50 mV) by 66.5±5.9% for WT (n=6, P<0.01 vs. control), 33.7±1.7% for Y90A (n=7, P<0.01 vs. WT), 34.0±6.0% for Y344A (n=5, P<0.01 vs. WT), 61.7±5.6% for Y376A (n=6, P=NS vs. WT), 67.9±7.8% for Y479A (n=5, P=NS vs. WT), 31.5±3.8% for Y485A (n=5, P<0.01 vs. WT), and 2.8±1.2% for triple mutant hEAG1 channels with Y90A, Y344A, and Y485A (n=5, P<0.01 vs. WT, Y376A, or Y479A; P<0.05 vs.Y90A, Y344A, or Y485A).

Fig. 8A illustrates the 50% concentrations (IC_{50}s) of AG556 for inhibiting WT and mutants of hEAG1 channels (at +50 mV). The IC_{50} was 6.1±1.2 μM (n=6) for WT, 6.7±1.1 μM for Y376A (n=6) and 5.8±1.2 μM for Y479A (n=5) (P=NS vs .WT). However, the IC_{50} was 16.8±0.9 μM for Y90A (n=7), 17.9±1.4 μM for Y344A (n=5), and 37.1±0.9 μM for Y485A (n=5, P<0.01 vs. WT, Y376A or A479A). The IC_{50} value for the triple mutant channel of Y90A, Y344A and Y485A cannot be obtained due to lack of sensitivity to AG556. These results indicate that three tyrosine residues, Tyr_{90}, Tyr_{344} and Tyr_{485}, but not Tyr_{376} and Tyr_{479}, are involved in tyrosine hosphorylation of hEAG1 channels. These three residues are located in different sections of hEAG1 channels. Y90 resides in the N-terminus of the hEAG1 channel and Y485 is located in the C-terminus while Y344 is in the cytoplasmic section between S4 and S5 (Fig. 8B).

4. Discussion

The present study demonstrates that the suppression of EGFR kinase with the selective inhibitor AG556, but not Src-family kinases with PP2, reduces hEAG1 current and tyrosine phosphorylation level in HEK 293 cells stably expressing hEAG1 gene. The inhibition is countered by the PTP inhibitor orthovanadate. Mutagenesis reveals that EGFR kinase likely regulates hEAG1 channels via phosphorylating the tyrosine residues Tyr_{90}, Try_{344} and Try_{485}.

4.1. Previous reports regarding hEAG1 channel regulation.

An earlier study reported that intracellular free Ca^{2+} was a negative regulator of rat EAG channel [29]. Recent reports have proved that calmodulin is the Ca^{2+} sensor for the modulation of hEAG1 channels [10,11]. In contrast to Ca^{2+}-activated potassium channels [33], hEAG1 channels are inhibited by Ca^{2+}/calmodulin via Ca^{2+} binding at the N- and C-termini [11]. However, cyclic AMP enhanced the EAG channel activity [1,2]. The proliferation of cancer cells is potentially modulated through the functionally expressed hEAG1 channels whose activities are regulated by Ca influx or K fluxes. Although it is well documented that PTKs participate in regulating ion channel activity [16,17], including several types of K^+ channels [16,34–36] and L-type Ca^{2+} channels [37,38], as well as volume sensitive Cl^- channels [23,39] in different types of cells, it is unknown whether there is potential modulation of hEAG1 channels by PTKs. The present study provides the novel information that hEAG1 channels are regulated by EGFR kinase, but not by Src-family kinases.

4.2. Novel findings of the present study

The potential regulation of ion channels by PTKs is generally based on the response to PTK inhibitors (e.g. AG556, PP2, etc.) and whether the effects induced by the PTK inhibitors can be countered by a PTP inhibitor [16,19,22,23,37]. We found that the highly selective EGFR kinase inhibitor AG556 [26] reversibly inhibited the hEAG1 current amplitude and modified the holding potential-dependent activation kinetics. The IC_{50} (6.1 μM) of AG556 for inhibiting WT hEAG1 channels is close to those of inhibiting EGFR kinase and cardiac I_{Na}

(7.6 μM) [22] or hERG channels (5.2 μM) [19]. However, the PDGFR kinase inhibitor AG1295 (10 μM) or the Src-family kinase inhibitor PP2 (10 μM) had no such effect, even at concentrations 20 times higher than IC_{50}s for inhibiting PDGFR kinase [27] or 2000 times higher than IC_{50}s for inhibiting Src-family kinases [28]. In addition, the PTP inhibitor orthovanadate significantly countered the reduced current amplitude and the modified holding potential-dependent activation kinetics by AG556. These results suggest that EGFR kinase, but not PDGRF kinase or Src-family kinases likely regulates hEAG1 channels. This is confirmed by the results with the immunoprecipitation and Western blot analysis: human EAG1 channel phosphorylation level was reduced by AG556, and the reduced phosphorylation is significantly countered by the PTP inhibitor orthovanadate. In addition, our experiment with EGFR siRNA showed a remarkable reduction of tyrosine phosphorylation level of hEAG1 channels, which further supports the notion that hEAG1 channels are regulated by EGFR kinase in hEAG1-HEK 293 cells.

Importantly, we found three tyrosine residues are located at Tyr_{90} in N-terminus, Try_{344} in cytoplasmic region between transmembranes S4 and S5, and Try_{485} in C-terminus are clearly responsible for the phosphorylation of the channels. The triple mutant sites Y90, Y344, and Y485 lack sensitivity to AG556, suggesting that Y90, Y344, and Y485 are responsible for tyrosine phosphorylation of hEAG1 by EGFR kinase.

4.3. Comparison with other ion channel regulation by PTKs

Basal tyrosine phosphorylation level of I_{Na} in guinea pig ventricular myocytes [22] and Kir2.3 channels expressed in HEK 293 cells [20] can be increased by the PTK activator EGF or the PTP inhibitor orthovanadate which significantly augments the current amplitude. However,
saturation of basal tyrosine phosphorylation is observed in Kir2.1 channels [21], hERG channels [19], KCNQ1/KCNE1 channels [18,40], cardiac native K^+ currents [34] and $I_{Ca.L}$ [37], in which the PTP inhibitor and/or EGF was unable to enhance the channel activity. These channels showed inhibitory response to PTK inhibitors, and the inhibition effect was significantly reversed by the PTP inhibitor orthovanadate [18,19,21,34,37]. In hERG channels, EGF or orthovanadate did not show any effect even with 36-h FBS-free (starvation) culture [19]. The hEAG1 channels, like hERG channels, showed no response to EGF or orthovanadate, even after a 36-h starvation, and was suppressed by the EGFR kinase inhibitor AG556, indicating a saturated level of basal tyrosine phosphorylation. Although both hEAG1 channels and hERG channels belong to the same superfamily of K^+ channels, the signal regulation may not be identical. A previous observation showed that hERG channel current, as $I_{Cl.vol}$ [23,41], was regulated by both Src-family kinases and EGFR kinase [19]. The present study demonstrated that hEAG1 channels, like cardiac I_{Na} [22] and I_{Ks} [18], were regulated only by EGFR kinase.

4.4. Significance and limitation of the present study.

Protein and mRNA of hEAG1 channels are expressed in many cancer cells, but not their corresponding normal tissues [3–6]. It has been reported that hEAG1 channels play a role in regulating proliferation of cancer cells. Silencing hEAG1 by RNA interference or hEAG1 channel inhibition by monoclonal antibody has been found to remarkably suppress cell proliferation and tumor progression [8,42]. The modulation of hEAG1 channels by EGFR kinase could therefore affect cell proliferation and tumor progression by changing membrane potential and intracellular Ca^{2+} levels. The inhibition of hEAG1 is at least partially responsible for the anticancer effect of specific EGFR kinase inhibitors [43–45]. In addition to the expression of hEAG1 channels in cancer cells, central neuronal cells highly express this channel [1,7]. Although the information regarding hEAG1 channel function under biological conditions is limited in neurons, hEAG1 channels may play a role in modulating neuronal activity [1,7]. Therefore, the regulation of hEAG1 channels by EGFR kinase could affect neuronal excitability.

One limitation of the present study was that we were unable to provide the data of phosphorylation level in mutant hEAG1 channels, because we had the difficulty in establishing the stable cell lines for this purpose, although it is ideal to demonstrate the reduced tyrosine phosphorylation level in the mutant channels.

Collectively, our study demonstrates for the first time that hEAG1 channels are regulated by EGFR kinase. Three tyrosine residues of the channels at different cytoplasmic regions of the hEAG1 channel (Tyr_{90}, Try_{344} and Try_{485}) are involved in phosphorylation with EGFR kinase, which may be involved in regulating tumor growth/migration and/or neuronal excitability.

Acknowledgement

The study was supported in part by a Small Project Fund (201007176213) of the University of Hong Kong and by Sun Chieh Yeh Heart Foundation of Hong Kong. Wei Wu is supported by a postgraduate studentship from the University of Hong Kong. Ming-Qing Dong is supported by a postdoctoral fellowship of the University of Hong Kong. The authors thank Dr. L Pardo, Max Planck Institute of Experimental Medicine, Göttingen, Germany, for generously providing us with the hEAGl/pTracer CMV plasmid.

References

[1] A. Bruggemann, L.A. Pardo, W. Stuhmer, O. Pongs, Ether-a-go-go encodes a voltage-gated channel permeable to K+ and Ca2+ and modulated by cAMP, Nature, 365 (1993) 445-448.

[2] J. Ludwig, H. Terlau, F. Wunder, A. Bruggemann, L.A. Pardo, A. Marquardt, W. Stuhmer, O. Pongs, Functional expression of a rat homologue of the voltage gated either a go-go potassium channel reveals differences in selectivity and activation kinetics between the Drosophila channel and its mammalian counterpart, EMBO J, 13 (1994) 4451-4458.

[3] L.M. Farias, D.B. Ocana, L. Diaz, F. Larrea, E. Avila-Chavez, A. Cadena, L.M. Hinojosa, G. Lara, L.A. Villanueva, C. Vargas, E. Hernandez-Gallegos, I. Camacho-Arroyo, A. Duenas-Gonzalez, E. Perez-Cardenas, L.A. Pardo, A. Morales, L. Taja-Chayeb, J. Escamilla, C. Sanchez-Pena, J. Camacho, Ether a go-go potassium channels as human cervical cancer markers, Cancer Res, 64 (2004) 6996-7001.

[4] B. Hemmerlein, R.M. Weseloh, F. Mello de Queiroz, H. Knotgen, A. Sanchez, M.E. Rubio, S. Martin, T. Schliephacke, M. Jenke, R. Heinz Joachim, W. Stuhmer, L.A. Pardo, Overexpression of Eag1 potassium channels in clinical tumours, Mol Cancer, 5 (2006) 41.

[5] F. Mello de Queiroz, G. Suarez-Kurtz, W. Stuhmer, L.A. Pardo, Ether a go-go potassium channel expression in soft tissue sarcoma patients, Mol Cancer, 5 (2006) 42.

[6] L.A. Pardo, C. Contreras-Jurado, M. Zientkowska, F. Alves, W. Stuhmer, Role of voltage-gated potassium channels in cancer, J Membr Biol, 205 (2005) 115-124.

[7] M.J. Saganich, E. Machado, B. Rudy, Differential expression of genes encoding subthreshold-operating voltage-gated K^+ channels in brain, J Neurosci, 21 (2001) 4609-4624.

[8] C. Weber, F. Mello de Queiroz, B.R. Downie, A. Suckow, W. Stuhmer, L.A. Pardo, Silencing the activity and proliferative properties of the human EagI Potassium Channel by RNA Interference, J Biol Chem, 281 (2006) 13030-13037.

[9] O. Gavrilova-Ruch, R. Schonherr, S.H. Heinemann, Activation of hEAG1 potassium channels by arachidonic acid, Pflugers Arch, 453 (2007) 891-903.

[10] R. Schonherr, K. Lober, S.H. Heinemann, Inhibition of human ether a go-go potassium channels by Ca(2+)/calmodulin, EMBO J, 19 (2000) 3263-3271.

[11] U. Ziechner, R. Schonherr, A.K. Born, O. Gavrilova-Ruch, R.W. Glaser, M. Malesevic, G. Kullertz, S.H. Heinemann, Inhibition of human ether a go-go potassium channels by Ca2+/calmodulin binding to the cytosolic N- and C-termini, FEBS J, 273 (2006) 1074-1086.

[12] Z. Wang, G.F. Wilson, L.C. Griffith, Calcium/calmodulin-dependent protein kinase II phosphorylates and regulates the Drosophila eag potassium channel, J Biol Chem, 277 (2002) 24022-24029.

[13] D.D. Marble, A.P. Hegle, E.D. Snyder, 2nd, S. Dimitratos, P.J. Bryant, G.F. Wilson, Camguk/CASK enhances Ether-a-go-go potassium current by a phosphorylation-dependent mechanism, J Neurosci, 25 (2005) 4898-4907.

[14] S.R. Hubbard, J.H. Till, Protein tyrosine kinase structure and function, Annu Rev Biochem, 69 (2000) 373-398.

[15] T. Hunter, Signaling--2000 and beyond, Cell, 100 (2000) 113-127.

[16] M.J. Davis, X. Wu, T.R. Nurkiewicz, J. Kawasaki, P. Gui, M.A. Hill, E. Wilson, Regulation of ion channels by protein tyrosine phosphorylation, Am J Physiol Heart Circ Physiol, 281 (2001) H1835-1862.

[17] I.B. Levitan, Modulation of ion channels by protein phosphorylation and dephosphorylation, Annu Rev Physiol, 56 (1994) 193-212.

[18] M.Q. Dong, H.Y. Sun, Q. Tang, H.F. Tse, C.P. Lau, G.R. Li, Regulation of human cardiac KCNQ1/KCNE1 channel by epidermal growth factor receptor kinase, Biochim Biophys Acta, 1798 (2010) 995-1001.

[19] D.Y. Zhang, Y. Wang, C.P. Lau, H.F. Tse, G.R. Li, Both EGFR kinase and Src-related tyrosine kinases regulate human ether-a-go-go-related gene potassium channels, Cell Signal, 20 (2008) 1815-1821.

[20] D.Y. Zhang, Y.H. Zhang, H.Y. Sun, C.P. Lau, G.R. Li, Epidermal growth factor receptor tyrosine kinase regulates the human inward rectifier potassium channel Kir2.3 stably expressed in HEK 293 cells, Br J Pharmacol, 164 (2011) 1469-1478

[21] D.Y.. Zhang, W. Wei, X.L. Deng, C.P. Lau, G.R. Li, Genistein and tyrphostin AG556 inhibit inwardly-rectifying Kir2.1 channels expressed in HEK 293 cells via protein tyrosine kinase inhibition, Biochimica et Biophysica Acta (BBA) - Biomembranes, 1808 (2011) 1993-1999.

[22] H. Liu, H.Y. Sun, C.P. Lau, G.R. Li, Regulation of voltage-gated cardiac sodium current by epidermal growth factor receptor kinase in guinea pig ventricular myocytes, J Mol Cell Cardiol, 42 (2007) 760-768.

[23] X.L. Du, Z. Gao, C.P. Lau, S.W. Chiu, H.F. Tse, C.M. Baumgarten, G.R. Li, Differential effects of tyrosine kinase inhibitors on volume-sensitive chloride current in human atrial myocytes: evidence for dual regulation by Src and EGFR kinases, J Gen Physiol, 123 (2004) 427-439.

[24] M.Q. Dong, C.P. Lau, Z. Gao, G.N. Tseng, G.R. Li, Characterization of recombinant human cardiac KCNQ1/KCNE1 channels (I (Ks)) stably expressed in HEK 293 cells, J Membr Biol, 210 (2006) 183-192.

[25] Q. Tang, M.W. Jin, J.Z. Xiang, M.Q. Dong, H.Y. Sun, C.P. Lau, G.R. Li, The membrane permeable calcium chelator BAPTA-AM directly blocks human ether a-go-go-related gene potassium channels stably expressed in HEK 293 cells, Biochem Pharmacol, 74 (2007) 1596-1607.

[26] A. Gazit, N. Osherov, I. Posner, P. Yaish, E. Poradosu, C. Gilon, A. Levitzki, Tyrphostins. 2. Heterocyclic and alpha-substituted benzylidenemalononitrile tyrphostins as potent inhibitors of EGF receptor and ErbB2/neu tyrosine kinases, J Med Chem, 34 (1991) 1896-1907.

[27] M. Kovalenko, A. Gazit, A. Bohmer, C. Rorsman, L. Ronnstrand, C.H. Heldin, J. Waltenberger, F.D. Bohmer, A. Levitzki, Selective platelet-derived growth factor receptor kinase blockers reverse sis-transformation, Cancer Res, 54 (1994) 6106-6114.

[28] J.H. Hanke, J.P. Gardner, R.L. Dow, P.S. Changelian, W.H. Brissette, E.J. Weringer, B.A. Pollok, P.A. Connelly, Discovery of a novel, potent, and Src family-selective tyrosine kinase inhibitor. Study of Lck- and FynT-dependent T cell activation, J Biol Chem, 271 (1996) 695-701.

[29] C.E. Stansfeld, J. Roper, J. Ludwig, R.M. Weseloh, S.J. Marsh, D.A. Brown, O. Pongs, Elevation of intracellular calcium by muscarinic receptor activation induces a block of voltage-activated rat ether-a-go-go channels in a stably transfected cell line, Proc Natl Acad Sci U S A, 93 (1996) 9910-9914.

[30] R. Schonherr, S. Hehl, H. Terlau, A. Baumann, S.H. Heinemann, Individual subunits contribute independently to slow gating of bovine EAG potassium channels, J Biol Chem, 274 (1999) 5362-5369.

[31] G.R. Li, H. Sun, X. Deng, C.P. Lau, Characterization of ionic currents in human mesenchymal stem cells from bone marrow, Stem Cells, 23 (2005) 371-382.

[32] H.K. Kramer, I. Onoprishvili, M.L. Andria, K. Hanna, K. Sheinkman, L.B. Haddad, E.J. Simon, Delta opioid activation of the mitogen-activated protein kinase cascade does not require transphosphorylation of receptor tyrosine kinases, BMC Pharmacol, 2 (2002) 5.

[33] C.M. Fanger, S. Ghanshani, N.J. Logsdon, H. Rauer, K. Kalman, J. Zhou, K. Beckingham, K.G. Chandy, M.D. Cahalan, J. Aiyar, Calmodulin mediates calcium-dependent activation of the intermediate conductance KCa channel, IKCa1, J Biol Chem, 274 (1999) 5746-5754.

[34] Z. Gao, C.P. Lau, T.M. Wong, G.R. Li, Protein tyrosine kinase-dependent modulation of voltage-dependent potassium channels by genistein in rat cardiac ventricular myocytes, Cell Signal, 16 (2004) 333-341.

[35] S. Missan, P. Linsdell, T.F. McDonald, Tyrosine kinase and phosphatase regulation of slow delayed-rectifier K+ current in guinea-pig ventricular myocytes, J Physiol, 573 (2006) 469-482.

[36] Z. Tiran, A. Peretz, B. Attali, A. Elson, Phosphorylation-dependent regulation of Kv2.1 Channel activity at tyrosine 124 by Src and by protein-tyrosine phosphatase epsilon, J Biol Chem, 278 (2003) 17509-17514.

[37] T. Ogura, L.M. Shuba, T.F. McDonald, L-type Ca2+ current in guinea pig ventricular myocytes treated with modulators of tyrosine phosphorylation, Am J Physiol, 276 (1999) H1724-1733.

[38] S. Wijetunge, J.S. Lymn, A.D. Hughes, Effect of inhibition of tyrosine phosphatases on voltage-operated calcium channel currents in rabbit isolated ear artery cells, Br J Pharmacol, 124 (1998) 307-316.

[39] A. Lepple-Wienhues, I. Szabo, U. Wieland, L. Heil, E. Gulbins, F. Lang, Tyrosine kinases open lymphocyte chloride channels, Cell Physiol Biochem, 10 (2000) 307-312.

[40] S. Missan, J. Qi, J. Crack, T.F. McDonald, P. Linsdell, Regulation of wild-type and mutant KCNQ1/KCNE1 channels by tyrosine kinase, Pflugers Arch, 458 (2009) 471-480.

[41] Z. Ren, C.M. Baumgarten, Antagonistic regulation of swelling-activated Cl- current in rabbit ventricle by Src and EGFR protein tyrosine kinases, Am J Physiol Heart Circ Physiol, 288 (2005) H2628-2636.

[42] D. Gomez-Varela, E. Zwick-Wallasch, H. Knotgen, A. Sanchez, T. Hettmann, D. Ossipov, R. Weseloh, C. Contreras-Jurado, M. Rothe, W. Stuhmer, L.A. Pardo, Monoclonal antibody blockade of the human Eag1 potassium channel function exerts antitumor activity, Cancer Res, 67 (2007) 7343-7349.

[43] S. Huang, E.A. Armstrong, S. Benavente, P. Chinnaiyan, P.M. Harari, Dual-agent molecular targeting of the epidermal growth factor receptor (EGFR): combining anti-EGFR antibody with tyrosine kinase inhibitor, Cancer Res, 64 (2004) 5355-5362.

[44] J. Li, Y. Li, Z.Q. Feng, X.G. Chen, Anti-tumor activity of a novel EGFR tyrosine kinase inhibitor against human NSCLC in vitro and in vivo, Cancer Lett, 279 (2009) 213-220.

[45] T. Okabe, I. Okamoto, S. Tsukioka, J. Uchida, T. Iwasa, T. Yoshida, E. Hatashita, Y. Yamada, T. Satoh, K. Tamura, M. Fukuoka, K. Nakagawa, Synergistic antitumor effect of S-1 and the epidermal growth factor receptor inhibitor gefitinib in non-small cell lung cancer cell lines: role of gefitinib-induced down-regulation of thymidylate synthase, Mol Cancer Ther, 7 (2008) 599-606.

Figure legends

Figure 1. Effect of AG556 on hEAG1 current. ***A.*** Time-course of hEAG1 current recorded in a representative cell with a 300-ms voltage step to +50 mV from a holding potential of –80 mV, then back –40 mV (inset) in the absence and presence of 10 μM AG556. Original current traces at corresponding time points are shown in the right of the panel. ***B***. Voltage-dependent hEAG1 current traces recorded in a typical experiment with 300-ms voltage steps from –80 mV to between –60 and +60 mV, then back to –40 mV (inset) under control conditions, in the presence of 10 μM AG556, and upon washout. C. *I-V* relationships of hEAG1 current (n = 6, **P<0.01 vs. control).

Figure 2. AG556 on holding potential-dependent kinetics of hEAG1 current. ***A.*** Normalized variables of hEAG1 current activation in the absence and presence of were fitted to the Boltzmann equation as described previously [18]. ***B.*** Holding potential-dependent hEAG1 current was recorded in a representative cell with 1-s conditioning holding potentials between –100 and –20 mV, then step (300-ms) to +50 mV (inset), in the absence and presence of 10 μM AG556. ***C.*** Time to 80% activation of hEAG1 current at conditioning holding potentials of –100 and –20 mV. AG556 reversibly reduced the time to 80% activation of the current (n=6, **P<0.01 vs. control).

Figure 3. AG1295 and PP2 on hEAG1 current. ***A.*** Voltage-dependent hEAG1 current traces recorded in a typical experiment with the voltage protocol as in Fig. 1B in the absence and presence of 10 μM AG1295. ***B.*** Voltage-dependent hEAG1 current traces recorded in a representative cell in the absence and presence of 10 μM PP2. ***C.*** Mean percentage values of hEAG1 current in the absence (control) and presence of AG1295 or PP2 (n=7-8, P=NS vs. control).

Figure 4. Effect of orthovanadate on AG556-induced hEAG1 reduction. **A.** Voltage-dependent hEAG1 current traces recorded in a typical experiment with the voltage protocol as in Fig. 1B in control, after the application of 10 μM AG556 or AG556 plus 1 mM orthovanadate. ***B.*** Time-course of hEAG1 current recorded in a representative cell with the voltage protocol shown in the left inset. The inhibition of hEAG1 current by AG556 was countered by orthovanadate. The original current traces at the corresponding time points are shown in the right. ***C***. Mean percentage values of hEAG1 current (+50 mV) in control, in the presence of 10 μM AG556, and AG556 plus 1 mM orthovanadate (OV). Inhibition of hEAG1 current by AG556 (n=8, **P<0.01 vs. control) was significantly antagonized by orthovanadate (n=8, ##P<0.01 vs. AG556 alone). ***D.*** Western blot image of EGFR protein in HEK 293 cells with and without hEAG1 gene expression.

Figure 5. Antagonism of AG556 effect on holding potential-dependent kinetics of hEAG1 current by orthovanadate. ***A.*** Normalized variables of hEAG1 current activation in the absence and presence of were fitted (n=5) to the Boltzmann equation as described previously [18]. ***B.*** Holding potential-dependent hEAG1 current was recorded in a typical experiment with the protocol as shown in Fig 4A in the absence and presence of 10 μM AG556 or AG556 plus 1 mM orthovanadate. ***C.*** Time to 80% activation of hEAG1 current at conditioning holding potentials between –100 and –20 mV. AG556 reversibly reduced the time to 80% activation of the current (n=6, **P<0.01 vs control, #P<0.01 vs AG556 alone).

Figure 6. Tyrosine phosphorylation levels of hEAG1 channels. ***A*** and ***B.*** Images of immunoprecipitation and Western blot for tyrosine phosphorylation level of hEAG1 channels in cells treated vehicle (control), 1 mM orthovanadate (OV), 10 μM AG556, AG556 plus orthovanadate, 10 μM PP2, or 100 ng/ml EGF. ***C.*** Images of immunoprecipitation and Western blot for tyrosine phosphorylation level of hEAG1 channels in cells transfected with control siRNA and EGFR siRNA, respectively (40 nM), ***D***. Mean values of the relative tyrosine phosphorylation level of hEAG1 channel protein in the cells treated with orthovanadate, AG556, AG556 plus orthovanadate, PP2, or EGF with the concentration as described in A (n=4-7 experiments, **P<0.01 vs. control; #P<0.05 vs AG556 alone), and in the cells transfected with control siRNA or EGFR siRNA (n=3, ##P<0.01 vs. control siRNA).

Figure 7. Effects of AG556 on WT and mutant hEAG1 channels. ***A.*** Voltage-dependent current traces recorded with the voltage protocol shown in the inset of Fig 1B in representative cells expressing WT, Y90A, Y344A, Y376A, Y479A, and Y485A, respectively, before and after application of 10 μM AG556. ***B.*** Voltage-dependent current traces recorded in a representative cell expressing the

triple mutant gene with Y90A, Y344A and Y485A before and after application of 10 μM AG556. ***C.*** Mean percentage values of hEAG1 channel current (+50 mV) of different mutants (n=5-7, **P<0.01 vs WT, #P<0.05 vs. Y90A, Y344A, or Y485A).

Figure 8. Concentration-dependent effects of AG556 on hEAG1 current. ***A.*** Concentration-response relationships of AG556 for inhibiting WT and mutant hEAG1 channel currents. Data were fitted to the Hill equation: $E=E_{max}/[1+(IC_{50}/C)^b]$, where E is the inhibition of hERG1 current in percentage at concentration C, E_{max} is the maximum inhibition, IC_{50} is the concentration for half-maximum inhibition, and b is the Hill coefficient. ***B.*** Schematic model for the regulation of hEAG1 channels by EGFR kinase. Tyrosine residues of the hEAG1 channels at Tyr^{90}, Tyr^{344} and Tyr^{485} (red), but not Tyr^{376} and Tyr^{479} are phosphorylated by EGFR kinase. AG556 inhibited EGFR kinase via reducing the channel phosphorylation, and the effect may be countered by orthovanadate through inhibiting the channel dephosphorylation.

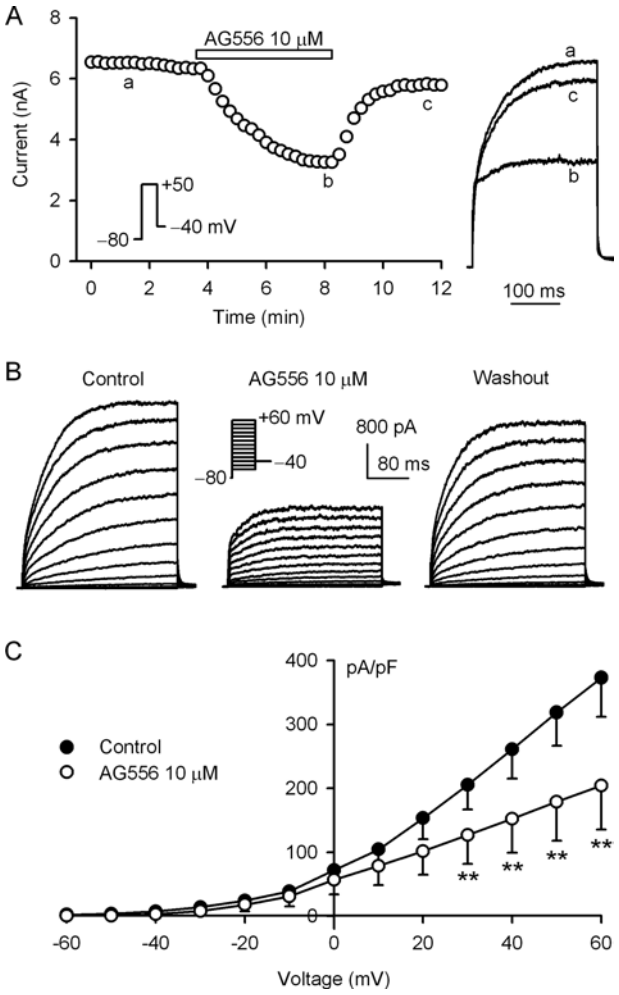
A
AG556 10 μM
Current (nA)
Time (min)
+50
−40 mV
−80
100 ms
B
Control
AG556 10 μM
Washout
+60 mV
−40
−80
800 pA
80 ms
C
pA/pF
Control
AG556 10 μM
Voltage (mV)

Figure 1

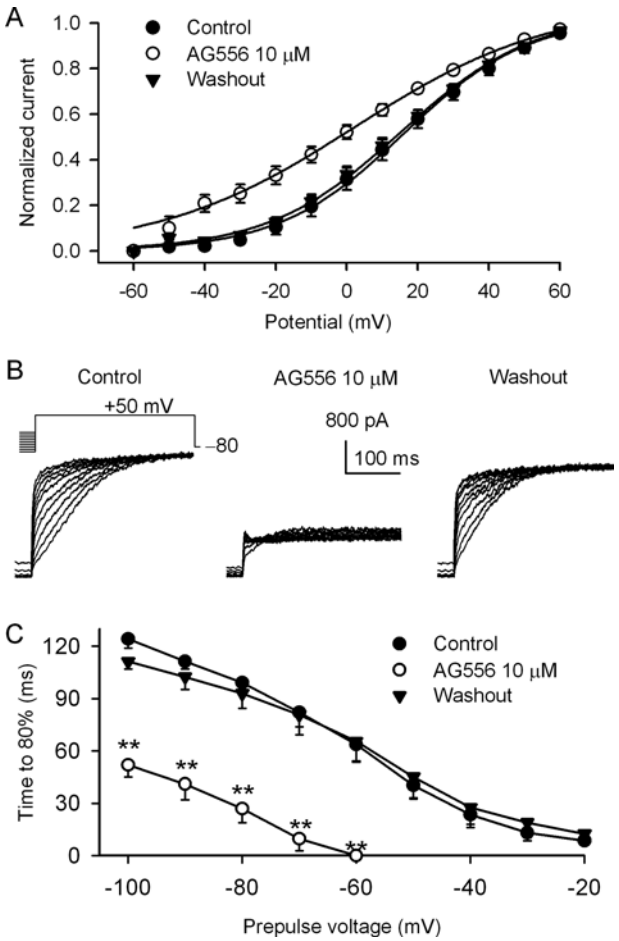
A
Control
AG556 10 μM
Washout
Normalized current
1.0
0.8
0.6
0.4
0.2
0.0
-60
-40
-20
0
20
40
60
Potential (mV)
B
Control
AG556 10 μM
Washout
+50 mV
-80
800 pA
100 ms
C
Control
AG556 10 μM
Washout
Time to 80% (ms)
120
90
60
30
0
**
-100
-80
-60
-40
-20
Prepulse voltage (mV)

Figure 2

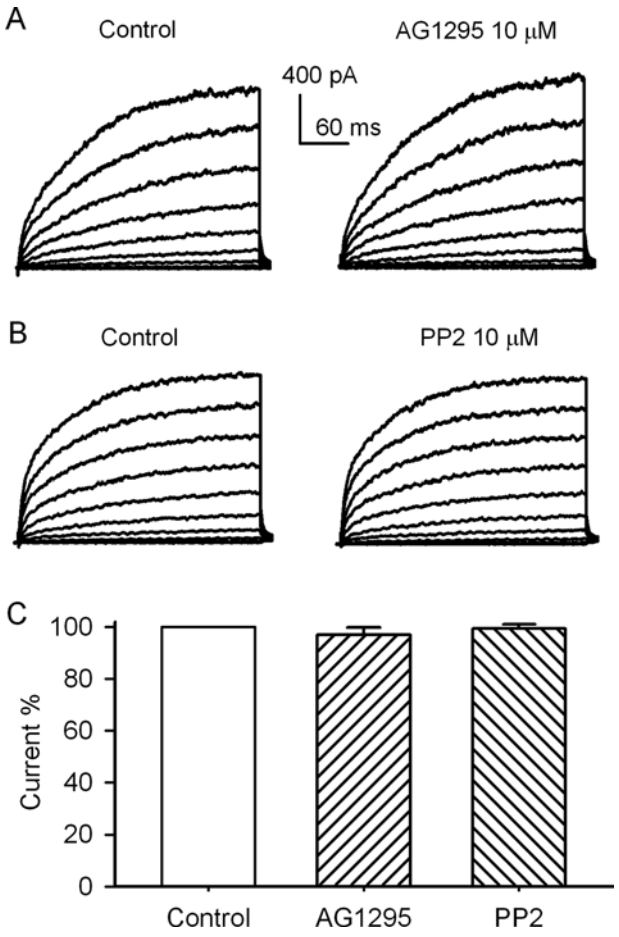
A
Control
AG1295 10 μM
400 pA
60 ms
B
Control
PP2 10 μM
C
Current %
100
80
60
40
20
0
Control
AG1295
PP2

Figure 3

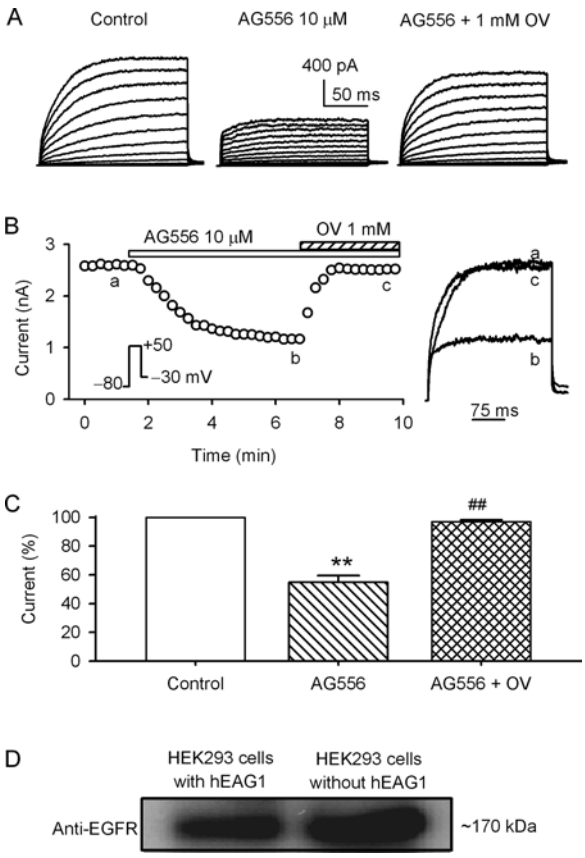
A
Control
AG556 10 μM
AG556 + 1 mM OV
400 pA
50 ms
B
AG556 10 μM
OV 1 mM
Current (nA)
Time (min)
+50
−30 mV
−80
a
b
c
75 ms
C
Current (%)
**
##
Control
AG556
AG556 + OV
D
HEK293 cells with hEAG1
HEK293 cells without hEAG1
Anti-EGFR
~170 kDa

Figure 4

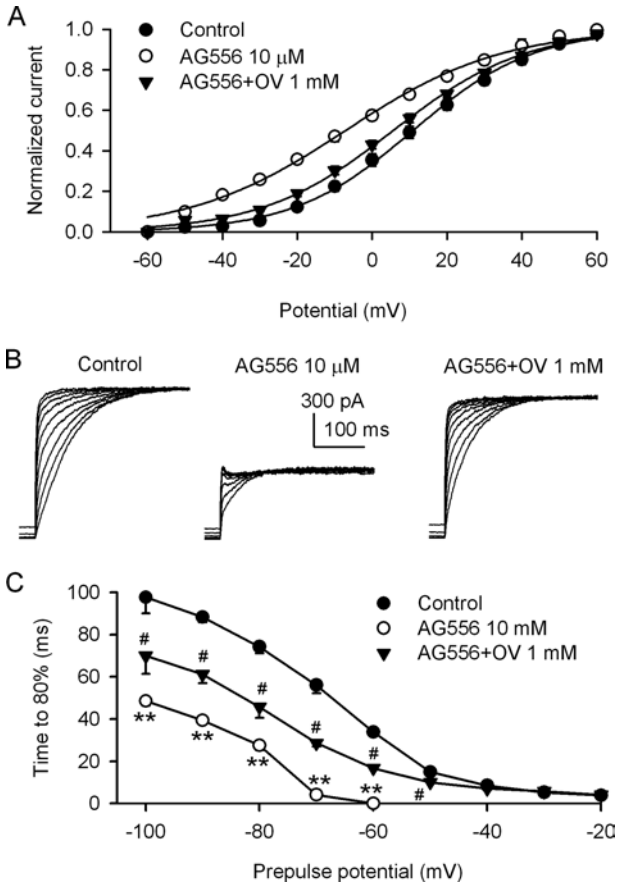
A
Control
AG556 10 μM
AG556+OV 1 mM
Normalized current
1.0
0.8
0.6
0.4
0.2
0.0
-60
-40
-20
0
20
40
60
Potential (mV)
B
Control
AG556 10 μM
AG556+OV 1 mM
300 pA
100 ms
C
Control
AG556 10 mM
AG556+OV 1 mM
Time to 80% (ms)
100
80
60
40
20
0
-100
-80
-60
-40
-20
Prepulse potential (mV)

Figure 5

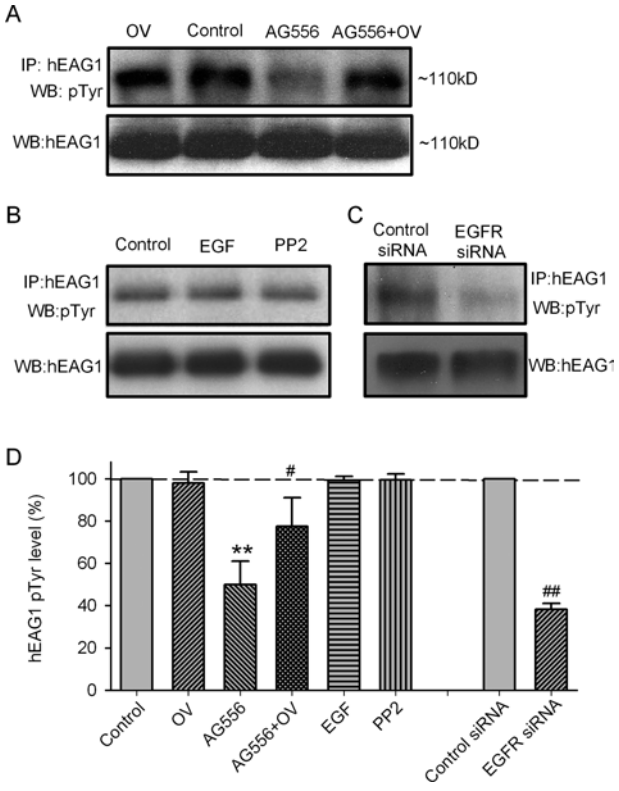
A
OV
Control
AG556
AG556+OV
IP: hEAG1
WB: pTyr
~110kD
WB:hEAG1
~110kD
B
Control
EGF
PP2
IP:hEAG1
WB:pTyr
WB:hEAG1
C
Control siRNA
EGFR siRNA
IP:hEAG1
WB:pTyr
WB:hEAG1
D
hEAG1 pTyr level (%)
100
80
60
40
20
0
**
#
##
Control
OV
AG556
AG556+OV
EGF
PP2
Control siRNA
EGFR siRNA

Figure 6

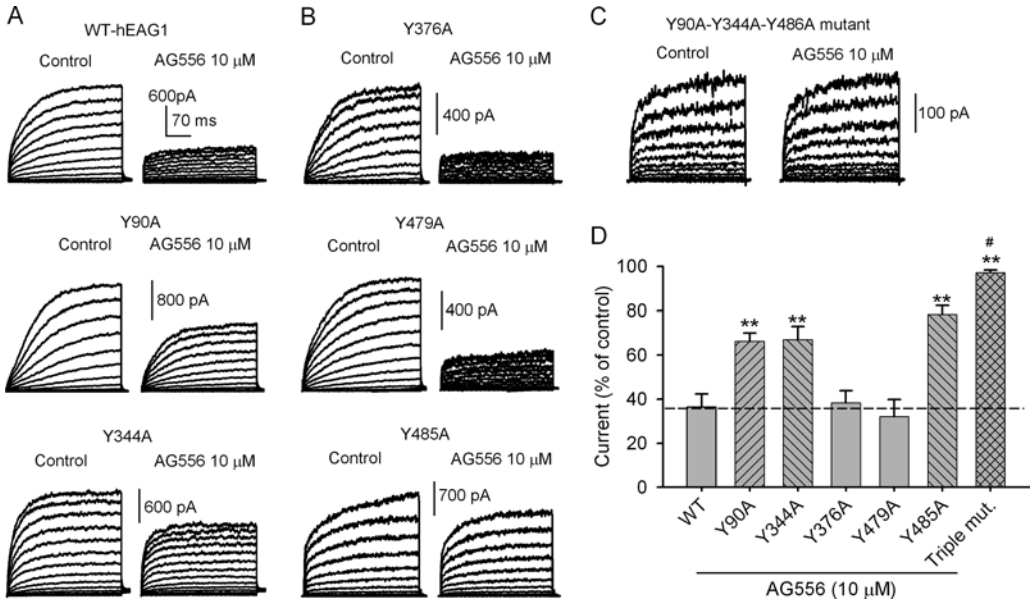
A
WT-hEAG1
Control
AG556 10 μM
600pA
70 ms
Y90A
Control
AG556 10 μM
800 pA
Y344A
Control
AG556 10 μM
600 pA
B
Y376A
Control
AG556 10 μM
400 pA
Y479A
Control
AG556 10 μM
400 pA
Y485A
Control
AG556 10 μM
700 pA
C
Y90A-Y344A-Y486A mutant
Control
AG556 10 μM
100 pA
D
Current (% of control)
100
80
60
40
20
0
**
**
**
**
#
WT
Y90A
Y344A
Y376A
Y479A
Y485A
Triple mut.
AG556 (10 μM)

Figure 7

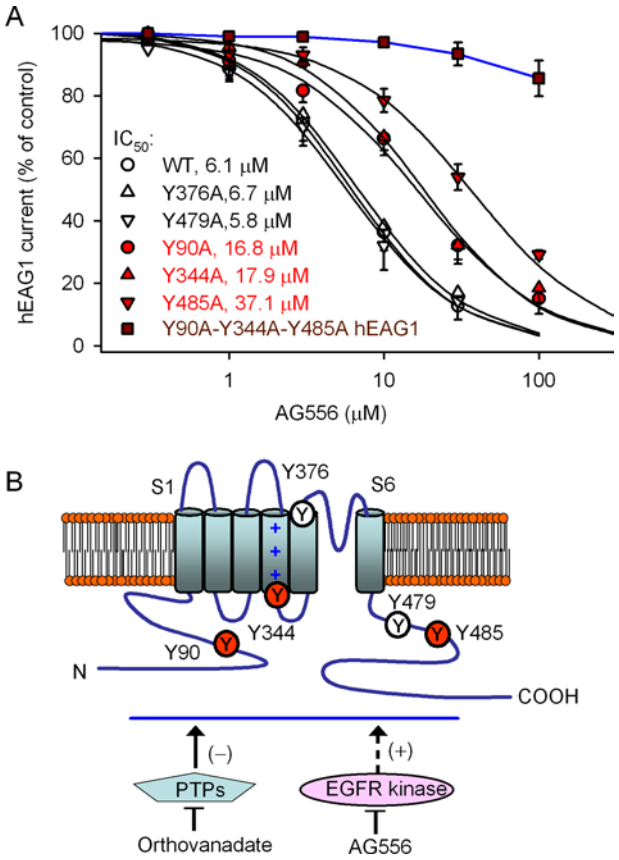
A
100
80
60
40
20
0
hEAG1 current (% of control)
IC50:
WT, 6.1 μM
Y376A,6.7 μM
Y479A,5.8 μM
Y90A, 16.8 μM
Y344A, 17.9 μM
Y485A, 37.1 μM
Y90A-Y344A-Y485A hEAG1
1
10
100
AG556 (μM)
B
S1
Y376
S6
Y479
Y344
Y485
Y90
N
COOH
(–)
(+)
PTPs
EGFR kinase
Orthovanadate
AG556

Figure 8